

# The structures of 1-chlorogermatrane and of 1-fluorogermatrane, revisited

Reint Eujen \*, Erwin Petrauskas, Achim Roth, David J. Brauer

*FB 9-Anorganische Chemie, Fachbereich 9, Bergische Universität-GH Wuppertal, Gaußstraße 20, D-42097 Wuppertal, Germany*

Received 16 March 2000; accepted 13 July 2000

Dedicated to Professor O. Stelzer on the occasion of his 60th birthday.

## Abstract

The crystal structures of 1-fluorogermatrane ( $P2_1$ ) and of the 1:3 acetonitrile adduct of 1-chlorogermatrane ( $P6_3$ ) have been determined by X-ray diffraction. A previously reported very short transannular Ge–N contact of 201.1(9) pm in 1-fluorogermatrane is corrected to 210.4(2) pm which complies well with the value of 209.6(3) pm found for the chloro analog. The structural parameters of both germatrane molecules are consistent with  $C_3$  symmetry. No indication was found for an unusually flexible cage or for an impact of the crystal packing on the Ge–N linkage. © 2000 Elsevier Science B.V. All rights reserved.

*Keywords:* Crystal structure; Germanium; Germatrane; Vibrational spectroscopy

## 1. Introduction

The transannular metal–nitrogen distance in metallatranes (1-metalla-2,8,9-trioxa-5-aza-bicyclo[3.3.3]undecane), especially in silatranes [1] and germatranes [2], has been subject to numerous experimental and theoretical studies. The most striking point in these investigations is the marked discrepancy between concurring theoretical calculations and crystal structure data. Rather independent of the chosen method, theory predicts a very shallow potential for the Si–N interaction in silatranes with equilibrium distances which are much longer than those found in the crystal structures [3,4], while they are much more compatible with the results of two high temperature electron diffraction studies [5]. Crystal packing forces have been made responsible for the significant bond shortening in the solid state [3].

In general, the M–N contact is influenced by the effective Lewis acidity of the metal, and the M–N distance may well be considered to reflect the electronic influence of the substituent on the metal. Recently, we have investigated the crystal structures of 1-trifl-

uoromethylsilatrane [6] and 1-trifluoromethylgermatrane [7] in order to confirm the pronounced electron-withdrawing capability of the  $CF_3$  group. As expected, the Si–N, 202.4(1) pm, and Ge–N contacts, 210.8(2) pm, were found to be much shorter than those of corresponding alkyl or aryl derivatives, and they are similar to those of the halogen substituted atranes. The difference of 8.4 pm between the sila and germa derivative for this dative interaction complies with a difference of 10.2 pm in covalent Si–N and Ge–N bond lengths [8]. In a recent paper a surprisingly short Ge–N contact has been claimed for 1-fluorogermatrane [9]. The reported distance of 201.1(9) pm obtained from a single crystal investigation was even shorter than that of the corresponding silatrane, 204.2(1) pm, and 8 pm shorter than that of 1-bromogermatrane [10]. A rationalization of the short Ge–N interaction based on crystal packing forces has appeared recently [11].

Despite the interest in the Ge–N bond length in 1-fluorogermatrane, the precision of its structure determination is only modest [9]. The standard deviations of the bond lengths involving the germanium atom lie in the 0.5–1.0 pm range, and the published C–O and C–N bond lengths both have a physically unrealistic spread of 7 pm. The latter variation is surprising for a com-

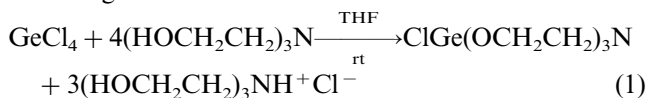
\* Corresponding author. Tel.: +49-202-4392503; fax: +49-202-4393052.

E-mail address: eujen@uni-wuppertal.de (R. Eujen).

pound of ideal  $C_3$  symmetry especially because the published equivalent isotropic displacement parameters are relatively low and give no indication of disorder. These observations prompted us to synthesize the compound and reinvestigate its structure. Furthermore, in order to gain additional information on the effect of the apical group on the Ge–N interaction, we have augmented the reinvestigation of 1-fluorogeratrane by a study of 1-chlorogeratrane.

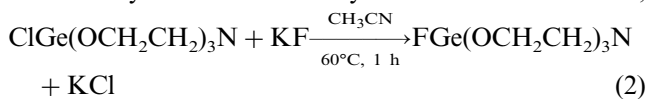
## 2. Results and discussion

1-Chlorogeratrane was obtained from  $\text{GeCl}_4$  and triethanolamine in tetrahydrofuran according to the following reaction:



Crystallization of the product from acetonitrile gave needles of the composition  $3\text{ClGe}(\text{OCH}_2\text{CH}_2)_3\text{N} \cdot \text{CH}_3\text{CN}$  which were suitable for X-ray structure analysis. Upon heating the solvent molecule is lost at  $99^\circ\text{C}$  while decomposition of the geratrane starts around  $300^\circ\text{C}$ .

Conversion of the chloride to the fluoride was achieved by reaction with anhydrous KF in acetonitrile,



The formation of the fluoride was monitored by  $^1\text{H}$ -NMR spectroscopy, the  $\text{OCH}_2$  resonance being readily identified by its small, but clearly detectable coupling (1.5 Hz) to the fluorine atom which had also been noted before [9]. The Ge–F bond was furthermore established by observation of the  $^1\text{H}$  decoupled  $^{19}\text{F}$ -NMR signal at  $-153.8$  ppm which showed the characteristic germanium isotope pattern with a Ge isotope shift of 1.4 ppb/mass unit.

### 2.1. Vibrational spectra

The infrared and Raman spectra of 1-fluoro- and 1-chlorogeratrane are listed in Table 1 together with the data of 1-trifluoromethylgeratrane for comparison. For the 12 non-hydrogen skeleton atoms 10  $a$  and 10  $e$  modes are expected for  $C_3$  symmetry, both being infrared and Raman active. For the atrane cage an assignment of particular modes in term of classical descriptions based on internal coordinates is hardly possible because similar force constants and atomic masses of the cage constituents imply extensive couplings. The general features of these spectra are very similar with a slight shift of most bands to higher wavenumbers for the fluoro derivative, and there are also great similarities with the spectra of silatranes [12].

In case of the acetonitrile adduct of the chlorogeratrane, the needle-like crystal shape allowed the distinction between vibrational modes which imply atomic motions mainly perpendicular to the molecular  $C_3$  axis and those with motions mainly parallel to this axis. With a  $90^\circ$  arrangement for laser and observation directions, the latter modes are observed when both incident laser beam and the direction of the observation are perpendicular to the needles. For example, the isolated CN stretch at  $2250\text{ cm}^{-1}$  of the acetonitrile molecules which are orientated perfectly parallel to the  $c$  axis is only observed with this orientation. Similarly, the intense Raman band at ca.  $615\text{ cm}^{-1}$  corresponds to a mode where the cage stretches preferentially along the  $C_3$  axis. In contrast, the second strong Raman emission in this region at ca.  $550\text{ cm}^{-1}$  becomes the most intense line by far when irradiated along the needle axis, and it is readily assigned to the perpendicular  $\nu_s$  ( $\text{GeO}_3$ ) stretch.

The GeX stretches of the pentacoordinated germanium are expected to appear at somewhat lower wavenumbers with regard to the  $a_1$  components of the respective  $\text{GeX}_4$  molecules, and assignments of the bands at  $340\text{ cm}^{-1}$  and  $220\text{ cm}^{-1}$  for  $\text{X} = \text{Cl}$  ( $a_1$   $\text{GeCl}_4$  at  $397\text{ cm}^{-1}$ ) and  $\text{CF}_3$  ( $a_1$   $\text{Ge}(\text{CF}_3)_4$  at  $232\text{ cm}^{-1}$  [13]), respectively, are straightforward. The GeF stretch is not clearly discernable but is presumably embedded in the rather complex band system around  $620\text{ cm}^{-1}$ .

Due to extensive couplings between the cage modes, a more or less clear classification of a band as Ge–N stretch is not possible. The relatively weak interaction between the Ge and N atoms implies a small force constant and thus a rather small contribution to the potential energy distribution. Consequently, it is embedded in modes which are best described as the symmetric deformations at the apical Ge and N atoms; e.g. the vibration around  $270\text{ cm}^{-1}$  ( $\text{X} = \text{F}, \text{CF}_3$ ), which is lowered to  $259\text{ cm}^{-1}$  for  $\text{X} = \text{Cl}$  by interaction with the GeCl stretch at  $340\text{ cm}^{-1}$ , will bear some Ge–N character along with contributions from the symmetric  $\text{GeO}_3$  deformation.

### 2.2. Crystal structures

Our structure of 1-fluorogeratrane is shown in Fig. 1. Although no crystallographic symmetry is imposed on the compound, the structural parameters show no serious deviations from  $C_3$  symmetry. Bond distances and angles have been average accordingly, and these results are compared with those of Lukevics et al. [9] in Table 2. The comparison shows that our standard deviations are lower by a factor of about four and that the spread in chemically equivalent structural details is generally much lower in our investigation. The higher precision of our study is mainly the result of employing more significant intensities (2212 vs. 732) in the refine-

ment — our data set extending to higher  $2\theta$  values ( $60^\circ$  rather than  $50^\circ$ ) and unlike that of Lukevics et al. including Friedel equivalents. While solutions of this germatrane are achiral, crystallization results in the spontaneous separation of chiral molecules; interestingly, the crystal examined by us is apparently composed of molecules having the opposite chirality and orientation with respect to the polar  $b$  axis than that studied by Lukevics et al.

Significant disagreement in the two structural determinations of 1-fluorogermatrane is found for the Ge–N

contact. Our value is 9.3(9) pm longer. Because of the higher precision and better internal consistency of the present study, these results should supersede those of the previous examination. Another statistically significant difference is the 3(1) pm shorter Ge–F bond length found by us.

The three five-membered Ge–O–C–C–N rings exhibit markedly similar deviations from planarity. According to a Cremer–Pople analysis [14], the averaged amplitude of puckering is 36(1) pm, and the average phase angle of  $94.2(12)^\circ$  for these rings lies closer to the  $90^\circ$

Table 1  
Vibrational spectra ( $\text{cm}^{-1}$ ) of 1-fluoro-, 1-chloro-, and 1-trifluoromethylgermatrane <sup>a</sup>

R = F		R = Cl		R = CF <sub>3</sub>		Assignment
Raman	IR	Raman <sup>b</sup>	IR	Raman	IR	
163 m		136 m	⊥			e ( $\rho$ GeX)
222 w		184 m	⊥		178 s	a
		245 w	⊥		220 s	a ( $\nu$ GeCF <sub>3</sub> )
273 m		259 m			245 w	e
		298 w			270 s	a ( $\delta_s$ GeO <sub>3</sub> )/ $\nu$ GeN
322 m		320 m	⊥	320 sh	327 m	e
		342 m		340 s		a ( $\nu$ GeCl)
423 w	422 w	422 w	⊥	420 w	421 w	e
		457 w		456 w	419 w	a
562 vs	557 m	554 vs	⊥	552 m	522 w	$\delta_{as}$ CF <sub>3</sub>
602 w	601 m	600 m	⊥	596 m	546 s	a ( $\nu_s$ GeO <sub>3</sub> )
621 s	621/615 s	616 s		614 s	600 sh	e
658/652 w	655 s	658/647 w	⊥	652 vs	613 s	a/ $\nu$ GeF
					637/646 s	e ( $\nu_{as}$ GeO <sub>3</sub> )
762 vw		763/757 w		758 vw	716 m	$\delta_s$ CF <sub>3</sub>
871 vw	872 w	871 vw		870 s		a
901 m	899 s	899 m		897 vs	870 w	e
932 m	930 s	930 m	⊥	929 s	871/864 w	a
	1024 s			1021 vs	905/896 m	a
1046/1041 vw	1042 m	1038 w	⊥	1035 s	933 m	e
1063/1056 vw	1065/1060 vs	1052 w	⊥	1055 vs	1023 s	e
1077/1073 vw	1072 vs	1069 vw	⊥	1060 vs, b	1039 s	e
1095 w	1095 s	1093 m		1093 s	1067 m	e
1158 w	1158 m	1157 w	⊥	1158 w	1067 vs	a/ $\nu_{as}$ CF <sub>3</sub>
					1098 w	
					1167 w	
					1163 w	
					1197 m	$\nu_s$ CF <sub>3</sub>
1241 m	1240 w	1239 m	⊥		1249 m	
1271 m	1271 s	1270 m	⊥	1271 s	1246 m	
1359/1346 vw	1344 w	1356 m		1358/1342 w	1277 s	1280/1270 m
1380 vw	1385/1370 w	1377 vw		1380/1367 w		
1457 m	1457 s	1455 m		1455 s	1456 m	1451 s
1486 m	1486 m	1480 m	⊥	1481 m	1486 s	1489 m
		2250 m		2250 m		
2888 s	2887 s	2885 s	⊥	2882 s	2890 s	$\nu$ C=N
2954 sh	2950 s, b	2946 m	⊥	2955 s, b	2951 s	2880 s
2964 s	2663 m	2956 m				2947 m
2989 m	2990 sh	2986 m	⊥	2986 m	2996 m	2993 m
3001 sh		3007 m	⊥	3008 w		

<sup>a</sup> Ref. [7].

<sup>b</sup> Intensities are given for powder. For single crystal studies, || denotes a vibrational motion mainly parallel to the molecular  $C_3$  axis (dominant Raman intensity with both irradiation and observation perpendicular to the needle axis), ⊥ perpendicular motion (dominant Raman intensity with irradiation along the needle axis).

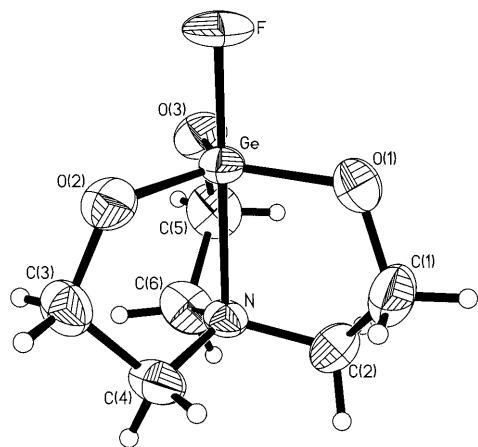


Fig. 1. A perspective drawing of 1-fluorogeriatrane using 50% probability thermal ellipsoids for the non-hydrogen atoms.

Table 2  
Comparison of bond lengths (pm) and angles ( $^{\circ}$ ) in 1-fluoro-, 1-chloro- and 1-trifluoromethylgeriatrane

X =	F <sup>a</sup>	F <sup>b</sup>	Cl	CF <sub>3</sub> <sup>c</sup>
Ge–X	175.1(2)	178.1(10)	220.9(1)	200.6(2)
Ge–N	210.4(2)	201.1(9)	209.6(3)	210.8(2)
Ge–O <sup>d</sup>	177.4(1)	176.7(11)	177.3(3)	178.7(3)
C–O <sup>d</sup>	141.9(5)	145.5(37)	141.5(3)	142.5(3)
C–C <sup>d</sup>	151.7(4)	152.1(15)	151.2(5)	151.6(4)
C–N <sup>d</sup>	147.3(3)	148.2(40)	148.0(4)	147.8(3)
O–Ge–O <sup>d</sup>	119.6(9)	120.0(6)	119.6(9)	119.5(11)
O–Ge–X <sup>d</sup>	93.7(5)	91.0(22)	93.5(4)	94.2(6)
O–Ge–N <sup>d</sup>	86.3(1)	89.0(15)	86.5(1)	85.8(1)
N–Ge–X	179.28(6)	179.1(5)	179.44(6)	179.18(7)
C–O–Ge <sup>d</sup>	115.4(4)	112.4(15)	114.6(4)	116.0(3)
C–C–O <sup>d</sup>	110.4(4)	109.9(8)	111.0(4)	109.9(2)
C–C–N <sup>d</sup>	107.7(2)	106.8(25)	107.1(4)	107.7(2)
C–N–Ge <sup>d</sup>	104.6(3)	105.9(14)	104.9(2)	104.4(2)
C–N–C <sup>d</sup>	113.9(5)	112.7(30)	113.6(6)	114.0(4)

<sup>a</sup> Present study.

<sup>b</sup> Ref. [9].

<sup>c</sup> Ref. [7].

<sup>d</sup> Value averaged assuming  $C_3$  symmetry with standard deviation taken as the larger of that determined from the spread or the average of the individual sigmas.

value of the canonical twist form than to the  $108^{\circ}$  phase of the canonical envelope form. The O–C–C–N fragments of these rings shows the greatest degree of torsion, the average angle being  $-44(1)^{\circ}$ .

1-Chlorogeriatrane cocrystallizes from acetonitrile in a 3:1 molar ratio with the solvent to form hexagonal crystals — the solvent molecule lying on the  $6_3$  axis and thus possessing crystallographic  $C_3$  symmetry. Although no crystallographic symmetry is imposed on the geriatrane (Fig. 2), its structural parameters comply well with  $C_3$  symmetry. The five-membered Ge–O–C–C–N rings assume a twist conformation with an average puckering amplitude and phase of  $36(1)$  pm and  $271.1(7)^{\circ}$ , respectively. The appropriately averaged

values for bond lengths and bond angles are compared with those of 1-fluorogeriatrane and 1-trifluoromethylgeriatrane [7] in Table 2. The difference in the Ge–F and Ge–Cl bond lengths,  $45.8(2)$  pm, is somewhat larger than the  $41.8$  pm difference in standard values for these bonds [8]. Excellent agreement is found for the remaining bond distances and angles; in particular, the Ge–N bond in the fluoro derivative is slightly ( $0.8(4)$  pm) but not significantly longer than that in the chloro analog, and almost identical to that of the CF<sub>3</sub> compound. Similar Ge–N bond lengths were also found in 1-isothiocyanatogeriatrane ( $208.1(5)$  pm [15]) and 1-bromogeriatrane ( $209$  pm [10]), for which no standard deviations were given. Slightly longer contacts were reported for O-bonded geriatrane ( $210$ – $215$  pm [16]) while the values for alkyl- or aryl-geriatrane vary typically between  $216$  and  $224$  pm [2,17]. A long Ge–N distance,  $224.2(2)$  pm, has been reported recently for the N(SiMe<sub>3</sub>)<sub>2</sub> derivative [18].

As mentioned in the introduction, the high flexibility found for the transannular contact in atranes by quantum mechanical studies has suggested that packing forces will have a significant effect on the metal–nitrogen separation in the solid state [3]. From the shapes of the thermal ellipsoids in Figs. 1 and 2, we can see that the atomic displacements along the Ge–N directions are low and by no means larger than the displacements along the covalent bonds in these structures. If the molecular potential for the Ge–N interaction is in fact as weak as implied by the theoretical studies, then packing forces must be the major factor contributing to the Ge–N potential in the crystals. While we find packing effects difficult to quantify, some aspects of the packing deserves consideration. In addition to van der Waals forces, dipole–dipole interactions should be important in crystals of these 1-halogeriatrane because they are expected to possess large dipole moments.

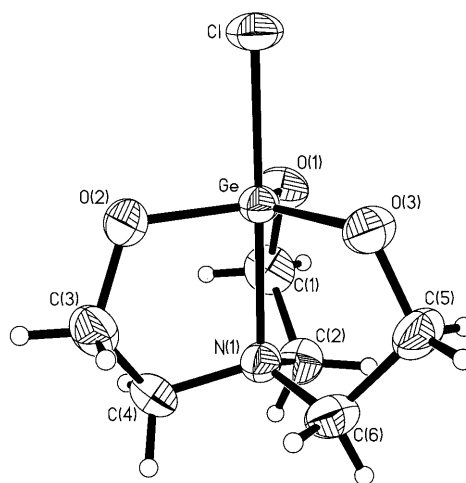


Fig. 2. A perspective drawing of 1-chlorogeriatrane using 50% probability thermal ellipsoids for the non-hydrogen atoms.

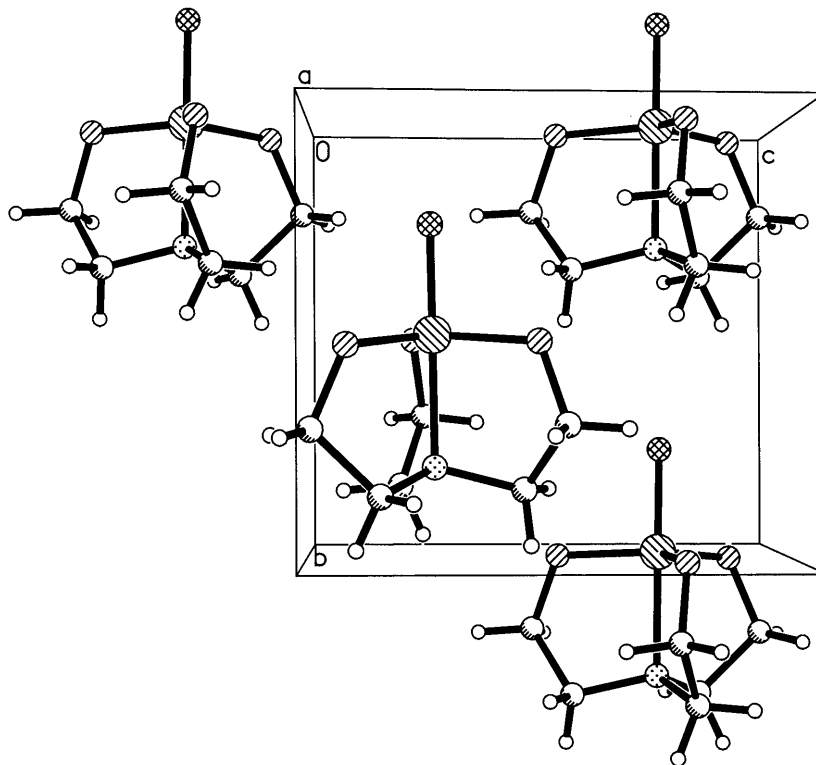


Fig. 3. A stripped-down view of the packing of 1-fluorogeratrane along the *b* axis.

These dipoles will be directed along their essentially linear N–Ge–X backbones; therefore, the relative orientation of the dipoles of neighboring molecules are important in the solid state. A stripped-down view of the surroundings of a 1-fluorogeratrane molecule is given in Fig. 3. It emphasizes the parallel alignment of the dipoles along the *b* axis and shows that the fluorine atom of one molecule nestles into the hollow of the N(CH<sub>2</sub>)<sub>3</sub> pyramid of the molecule above it. This packing mode appears to be quite efficient. From a molecular volume of 0.1585 nm<sup>3</sup>, which can be calculated from the atomic coordinates (hydrogen atoms idealized) and standard van der Waals radii [19], we obtain a packing coefficient of 0.755, which lies at the upper end of the range (0.65–0.75) found for molecular crystals [20]. A variant of this packing is found in cocrystals of 1-chlorogeratrane and acetonitrile. Here a head-to-tail alignment of the N–Ge–Cl fragments occurs parallel to the hexagonal *c* axis (Fig. 4). That this *c* axis is 79.6(2) pm longer than the *b* axis of 1-fluorogeratrane is largely accounted for by the difference in the Ge–F and Ge–Cl interatomic distances (45.8(2) pm) plus the 28 pm larger van der Waals radius of chlorine vs. fluorine. From the molecular volumes of 1-chlorogeratrane (0.1679 nm<sup>3</sup>) and acetonitrile (0.0451 nm<sup>3</sup>) calculated as described above, we estimate a packing coefficient of 0.728 which is somewhat less than that obtained for 1-fluorogeratrane. Specific interactions between the acetonitrile and 1-chlorogeratrane molecules are not

strong — the contact delineated in Fig. 4 between the methyl hydrogen and an oxygen atom of 234(5) pm [21] being at best a feeble hydrogen bond [22].

### 3. Experimental

Chemicals were obtained from commercial sources and used without further purification. Raman spectra were obtained on a Cary 82 spectrometer with Kr<sup>+</sup> excitation at 647 nm and a Bruker Equinox55 equipped with a Raman module and NdYAG excitation at 1064 nm. Infrared spectra were recorded with a Bruker IFS 25 spectrometer as KBr pellets. Combined calorimetric and thermogravimetric analyses (DSC/TGA) were made with a simultaneous DSC/TG instrument, Netzsch STA 409. NMR spectra were recorded with a Bruker ARX 400 instrument (<sup>1</sup>H, 400.13 MHz; <sup>19</sup>F, 376. MHz; <sup>13</sup>C, 62.90 MHz) and referenced to internal DMSO-*d*<sub>6</sub> at 2.58 ppm (<sup>1</sup>H) and 39.50 ppm (<sup>13</sup>C), and external CFCl<sub>3</sub> (<sup>19</sup>F).

#### 3.1. 1-Chlorogeratrane

To 10.7 g (50 mmol) of GeCl<sub>4</sub> in 50 ml of THF was added slowly 30 g of N(CH<sub>2</sub>CH<sub>2</sub>OH)<sub>3</sub> (0.2 mol) in 50 ml of THF. The reaction mixture was stirred for 2 h at ambient temperature. The white precipitate was filtered off, extracted with hot acetonitrile and recrystallized

from acetonitrile which yielded 8.2 g (65%) of 1-chlorogeratrane. EIMS:  $m/z$  (rel. int.) 255 [6%,  $M^+$ ], 225 [100%,  $M^+ - CH_2O$ ], 220 [10%,  $M^+ - Cl$ ], 195 [39%,  $M^+ - 2CH_2O$ ]. Anal. Calc. for  $3C_6H_{12}ClGeNO_3 \cdot C_2H_3N$ : C, 29.89; H, 4.89; N, 6.97. Found: C, 29.6; H, 4.8; N, 6.7%.

### 3.2. 1-Fluorogeratrane

A suspension of 0.5 g chlorogeratrane and 1 g of dry KF in 5 ml of  $CH_3CN$  was stirred for 1 h at 60°C. The completion of the reaction was monitored by  $^1H$ -NMR spectroscopy. After hot filtration and evaporation of the solvent, the solid residue was recrystallized from acetonitrile. EIMS:  $m/z$  (rel. int.) 239 [7%,  $M^+$ ], 218 [14%,  $M^+ - F$ ], 209 [100%,  $M^+ - CH_2O$ ], 179 [67%,  $M^+ - 2CH_2O$ ].

### 3.3. X-ray structural investigations

Crystals of the geratrane were grown from acetonitrile solutions and were glued to glass fibers. X-ray data were collected with a Siemens P3 diffractometer employing Mo- $K_\alpha$  radiation and a graphite monochromator. Intensities were derived from the profiles of  $2\theta/\theta$  scans and were corrected for absorption. The

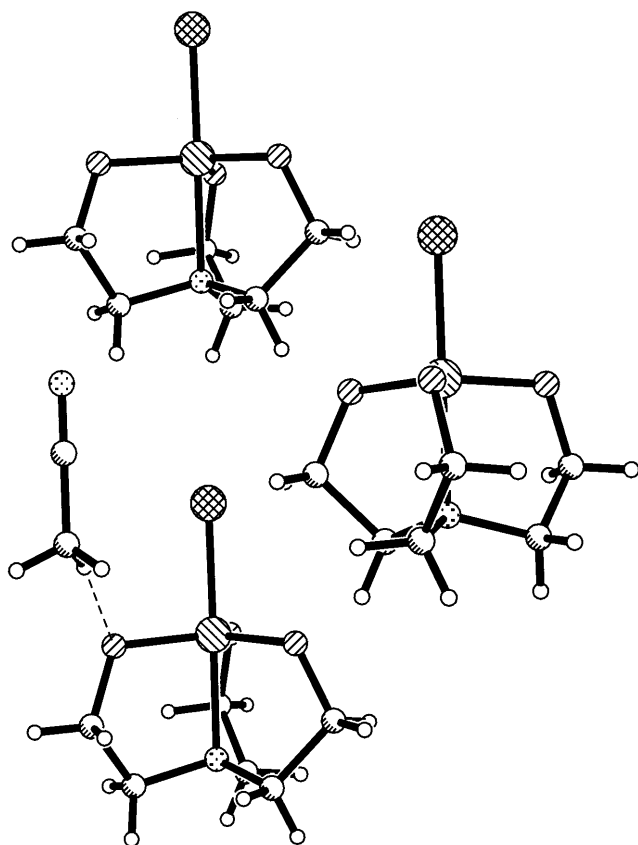


Fig. 4. The relative positions of the molecules along the  $c$  axis (vertical) in 1-chlorogeratrane·1/3acetonitrile.

Table 3  
Crystal data for 1-fluoro- and 1-chlorogeratrane

Empirical formula	$C_6H_{12}FGeNO_3$	$C_6H_{12}ClGeNO_3 \cdot 1/3C_2H_3N$
Formula weight	237.76	267.89
Crystal system	Monoclinic	Hexagonal
Space group	$P2_1$	$P6_3$
$a$ (Å)	7.1904(14)	14.680(2)
$b$ (Å)	7.285(2)	14.680(2)
$c$ (Å)	8.032(2)	8.081(2)
$\alpha$ (°)	90	90
$\beta$ (°)	93.75(2)	90
$\gamma$ (°)	90	120
$V$ (Å <sup>3</sup> )	419.83(14)	1508.0(4)
$Z$	2	6
$D_{calc}$ (g cm <sup>-3</sup> )	1.881	1.770
Wavelength (Å)	0.71073	0.71073
$T$ (K)	293(2)	294(2)
$\theta$ Range (°)	2.54–30.06	2.78–27.53
Limiting indices	$-10 \leq h \leq 10$ , $-10 \leq k \leq 10$ , $-11 \leq l \leq 11$	$-19 \leq h \leq 19$ , $-19 \leq k \leq 19$ , $-10 \leq l \leq 10$
Reflections collected	7950	7745
Unique	2473	2330
$R_{int}$	0.0217	0.0275
Observed ( $I > 2\sigma$ )	2212	1869
Crystal size (mm)	0.50 × 0.23 × 0.11	0.48 × 0.36 × 0.29
$\mu$ (mm <sup>-1</sup> )	3.632	3.289
Transmission	0.6989–0.4233	0.5785–0.5075
$R_1$ (all data)	0.0235	0.0278
$wR_2$ (all data)	0.0431	0.0392
Goodness-of-fit on $F^2$	0.992	0.980
Parameters	121	135
$\Delta F$ map (e Å <sup>-3</sup> )	0.285 to -0.279	0.227 to -0.163
Flack parameter	0.002(9)	-0.017(8)
Extinction coefficient		0.0152(4)

structures were solved by direct methods and were refined by least-squares techniques using a SHELXTL program package [23]. All hydrogen atoms were idealized except for that of the acetonitrile molecule, which was refined freely. Values determined for the Flack  $x$  parameter [24] lie close to zero which indicates that the absolute structures have been assigned correctly. Crystal data are given in Table 3, and the coordinates of the non-hydrogen atoms are collected in Tables 4 and 5.

## 4. Supplementary material

Crystallographic data (excluding structure factors) have been deposited with the Cambridge Crystallographic Data Centre as supplementary publication no. CCDC-145158 and CCDC-145159 for the chloro and fluoro derivatives, respectively. Copies of the data can be obtained free of charge on application to CCDC, 12

Table 4

Atomic coordinates and equivalent isotropic displacement parameters<sup>a</sup> (Å<sup>2</sup>) for FGe(OCH<sub>2</sub>CH<sub>2</sub>)<sub>3</sub>N

	x	y	z	U <sub>eq</sub>
Ge	0.69726(2)	0.4992	0.25828(2)	0.0324(1)
F	0.7030(3)	0.2589(3)	0.2543(2)	0.0630(7)
O(1)	0.7924(2)	0.5138(4)	0.4671(2)	0.0515(4)
O(2)	0.8424(2)	0.5234(3)	0.0894(2)	0.0458(4)
O(3)	0.4516(2)	0.5074(5)	0.2200(2)	0.0470(3)
N	0.6867(3)	0.7878(3)	0.2623(2)	0.0313(5)
C(1)	0.8507(4)	0.6925(4)	0.5197(3)	0.0594(7)
C(2)	0.7210(4)	0.8358(3)	0.4399(3)	0.0506(6)
C(3)	0.8482(3)	0.7025(3)	0.0201(3)	0.0472(5)
C(4)	0.8346(4)	0.8460(3)	0.1555(3)	0.0456(5)
C(5)	0.3680(3)	0.6806(4)	0.2411(3)	0.0553(6)
C(6)	0.4977(3)	0.8344(3)	0.1940(3)	0.0500(6)

<sup>a</sup> U<sub>eq</sub> is defined as one third of the trace of the orthogonalized U<sub>ij</sub> tensor.

Table 5

Atomic coordinates and equivalent isotropic displacement parameters<sup>a</sup> (Å<sup>2</sup>) for ClGe(OCH<sub>2</sub>CH<sub>2</sub>)<sub>3</sub>N·1/3CH<sub>3</sub>CN

	x	y	z	U <sub>eq</sub>
Ge	0.26721(1)	0.90993(2)	0.94735(5)	0.0278(1)
Cl	0.26877(9)	0.90817(10)	1.22063(9)	0.0469(3)
O(1)	0.18655(11)	0.96828(11)	0.9373(3)	0.0406(3)
O(2)	0.20676(11)	0.77119(11)	0.9334(4)	0.0417(4)
O(3)	0.40557(10)	0.99014(12)	0.9313(4)	0.0430(4)
N(1)	0.2647(3)	0.9100(3)	0.6880(3)	0.0309(8)
C(1)	0.1432(2)	0.9636(2)	0.7791(3)	0.0444(6)
C(2)	0.2192(2)	0.9768(2)	0.6436(3)	0.0389(6)
C(3)	0.2079(2)	0.7322(2)	0.7742(3)	0.0458(6)
C(4)	0.1973(2)	0.7987(2)	0.6409(3)	0.0389(6)
C(5)	0.4419(2)	1.0340(2)	0.7721(3)	0.0468(7)
C(6)	0.3766(2)	0.9561(2)	0.6386(3)	0.0410(6)
N(2)	0.3333	0.6667	0.4640(12)	0.100(2)
C(7)	0.3333	0.6667	0.3280(7)	0.0564(14)
C(8)	0.3333	0.6667	0.1507(9)	0.066(2)

<sup>a</sup> U<sub>eq</sub> is defined as one third of the trace of the orthogonalized U<sub>ij</sub> tensor.

Union Road, Cambridge CB2 1EZ, UK (fax: int. code + 44(1223)336-033; e-mail: deposit@ccdc.cam.ac.uk or www: http://www.ccdc.cam.ac.uk).

## Acknowledgements

Financial support by the Fond der Chemischen Industrie is gratefully acknowledged.

## References

- [1] E. Lukevics, O.A. Pudova, Chem. Heterocyclic Compd. 32 (1996) 1381.
- [2] Gmelin Handbook of Inorganic and Organometallic Chemistry, Syst. No. 45, Ge–Organogermanium Compounds, Part 5, Springer, Berlin, 1993, p. 319.
- [3] M.W. Schmidt, T.L. Windus, M.S. Gordon, J. Am. Chem. Soc. 117 (1995) 7480.
- [4] (a) J.E. Boggs, C. Peng, V.A. Pstunovich, V.F. Sidorkin, J. Mol. Struct. 357 (1995) 67. (b) T. Dahl, P.N. Skancke, Int. J. Quant. Chem. 60 (1996) 566. (c) G.I. Csonka, P. Hencsei, J. Comput. Chem. 17 (1996) 767. (d) G.I. Csonka, P. Hencsei, J. Mol. Struct. 362 (1996) 199.
- [5] (a) L. Parkanyi, P. Hencsei, L. Bihatsi, T. Müller, J. Organomet. Chem. 269 (1984) 1. (b) G. Forgacs, M. Kolonits, I. Hargittai, Struct. Chem. 1 (1989) 245.
- [6] R. Eujen, A. Roth, D.J. Brauer, Monatsh. Chem. 130 (1999) 109.
- [7] R. Eujen, A. Roth, D.J. Brauer, Monatsh. Chem. 130 (1999) 1341.
- [8] R. Blom, A. Haaland, J. Mol. Struct. 128 (1985) 21.
- [9] E. Lukevics, S. Belyakov, P. Arsenyan, J. Popelis, J. Organomet. Chem. 549 (1997) 163.
- [10] S.N. Gurkova, A.I. Gusev, V.A. Sharapov, N.V. Alekseev, T.K. Gar, N.J. Chromova, J. Organomet. Chem. 268 (1984) 119.
- [11] S. Belyakov, E. Lukevics, L. Ignatovich, J. Organomet. Chem. 577 (1999) 205.
- [12] (a) M. Imbenotte, G. Palavit, P. Legrand, J.P. Huvenne, G. Fleury, J. Mol. Spectrosc. 102 (1983) 40. (b) M. Imbenotte, G. Palavit, P. Legrand, J. Raman Spectrosc. 14 (1983) 135.
- [13] R. Eujen, H. Bürger, Spectrochim. Acta A 35 (1979) 541.
- [14] D. Cremer, J.A. Pople, J. Am. Chem. Soc. 97 (1975) 1354.
- [15] P. Narula, S. Soni, R. Shankar, R.K. Chadha, J. Chem. Soc. Dalton Trans. (1992) 3055.
- [16] (a) E. Lukevics, S. Belyakov, L. Ignatovich, N. Shilina, Bull. Soc. Chim. Fr. 132 (1995) 545. (b) G.S. Zaitseva, M. Nasim, L.I. Livantsova, V.A. Tafeenko, L.A. Aslanov, V.S. Petrosyan, Heteroatom. Chem. 1 (1990) 439.
- [17] (a) L.O. Atovmyan, Ya.Ya. Bleidelis, A.A. Kemme, R.P. Shivaeva, J. Struct. Chem. 11 (1970) 295. (b) S.N. Gurkova, A.I. Gusev, V.A. Sharapov, N.V. Alekseev, T.K. Gar, N.J. Chromova, J. Organomet. Chem. 268 (1984) 119. (c) G.S. Zaitseva, S.S. Karlov, A.V. Churakov, J.A.K. Howard, E.V. Avtomonov, J. Lorberth, Z. Anorg. Allg. Chem. 623 (1997) 1144. (d) G.S. Zaitseva, L.I. Livantsova, M. Nasim, S.S. Karlov, A.V. Churakov, J.A.K. Howard, E.V. Avtomonov, J. Lorberth, Chem. Ber. Recueil 130 (1997) 739. (e) G.S. Zaitseva, S.S. Karlov, E.S. Alekseyeva, L.A. Aslanov, E.V. Avtomonov, J. Lorberth, Z. Naturforsch. Teil. B 52 (1997) 30.
- [18] S.N. Nikoieva, K. Megges, J. Lorberth, V.S. Petrosyan, Z. Naturforsch. Teil B 53 (1998) 973.
- [19] A. Bondi, J. Phys. Chem. 68 (1964) 441.
- [20] A.I. Kitaigorodsky, Molecular Crystals and Molecules, Academic, New York, 1973.
- [21] With the C(8)–H(8) bond of the acetonitrile molecule extended to 109.6 pm, we calculate an H(8)⋯O(2) (y – x, 1 – x, z – 1) contact of 234(5) pm.
- [22] R. Taylor, O. Kennard, J. Am. Chem. Soc. 104 (1982) 5063.
- [23] G.M. Sheldrick, SHELXTL PC Version 5.03: An Integrated System for Solving, Refining and Displaying Crystal Structures from Diffraction Data, Siemens Analytical X-ray Instruments Inc., Madison, WI, 1994.
- [24] H.D. Flack, Acta Crystallogr. Sect. A 39 (1983) 876.